

Excited bottomonia in quark-gluon plasma from lattice QCD

Rasmus Larsen^{a,*}, Stefan Meinel^{b,c}, Swagato Mukherjee^a, Peter Petreczky^a

^a*Physics Department, Brookhaven National Laboratory, Upton, NY 11973, USA*

^b*Department of Physics, University of Arizona, Tucson, Arizona 85721, USA*

^c*RIKEN-BNL Research Center, Brookhaven National Laboratory, Upton, NY 11973, USA*

Abstract

We present the first lattice QCD study of up to $3S$ and $2P$ bottomonia at non-zero temperatures. Correlation functions of bottomonia were computed using novel bottomonium operators and a variational technique, within the lattice non-relativistic QCD framework. We analyzed the bottomonium correlation functions based on simple physically-motivated spectral functions. We found evidence of sequential in-medium modifications, in accordance with the sizes of the bottomonium states.

Keywords: Heavy-ion collision, Quark-gluon plasma, Quarkonium, Lattice QCD

1. Introduction

Quarkonium suppression has been proposed as a signature of quark-gluon plasma (QGP) formation in heavy-ion collisions [1]. The main idea behind this proposal was the observation that color screening within a deconfined medium can make the interaction between the heavy quark and anti-quark short ranged, leading to the dissolution of quarkonia in QGP. At a given temperature, different quarkonium states are expected to be affected differently by QGP—a more tightly bound quarkonia having a smaller size is less influenced by the medium than a relatively loosely bound, larger one. Therefore, following the hierarchy of their binding energy and sizes, a sequential pattern of in-medium modification is expected [2, 3]. Some evidence of sequential in-medium modification of quarkonia comes from lattice QCD studies of S-wave and P-wave quarkonium correlators along the temporal [4–8] and spatial [9, 10] directions. Recent studies have revealed that inclusion of dissipative effects lead to a more complex theoretical picture of in-medium heavy quark and anti-quark interactions [11, 12]. However, the main conclusion, i.e., that quarkonium dissolve in QGP when the temperature is large enough compared to its inverse size and binding energy, have remained unchanged [13–17]. Hints for sequential in-medium modification of bottomonia have also been observed in heavy-ion collision experiments [18–22]. While the connection between the observed hierarchy of the $\Upsilon(nS)$ yields in heavy-ion collisions and the expected sequential melting of these states in QGP is complicated

by dynamical effects, such a link is expected to exist [23–25]. For this reason, the study of sequential in-medium quarkonium modifications in heavy-ion collisions is a subject of extensive experimental and theoretical efforts; for recent reviews see Refs. [26, 27].

There have been many attempts to study in-medium properties of charmonium [28–36] and bottomonium [4–8, 33, 37, 38] in lattice QCD, almost entirely focused on in-medium modifications of ground states of S- and P-wave quarkonium. Previous lattice QCD studies of in-medium quarkonium used point meson operators, i.e., operators with quark and anti-quark fields located in the same spatial point, which are known to have non-optimal overlap with the quarkonium wave-functions, especially, with the excited states. As a result, these correlators are largely dominated by the vacuum continuum parts of the spectral function, and isolating the contributions of in-medium bottomonium becomes quite difficult [16, 17, 39]. Recently, we explored the possibility of studying in-medium bottomonium properties using correlators of extended meson operators [40]. We found that such operators have very good overlap with the lowest S- and P-state bottomonia, thereby allowing us to cleanly isolate the vacuum continuum contributions to the bottomonium correlators. We showed that these correlators are more sensitive to the in-medium bottomonium properties than the ones with point sources. Analyzing these correlators, we found evidence for thermal broadening of the $1S$ - and $1P$ -state bottomonia, however, excited bottomonium states remained elusive. In this letter we introduce novel extended meson operators within the lattice non-relativistic QCD (NRQCD) formalism, which, for the first time, allow us to probe in-medium modifications of up to $3S$ and $2P$ bottomonium.

*Corresponding author

Email addresses: rlarsen@bnl.gov (Rasmus Larsen), smeinel@email.arizona.edu (Stefan Meinel), swagato@bnl.gov (Swagato Mukherjee), petreczk@quark.phy.bnl.gov (Peter Petreczky)

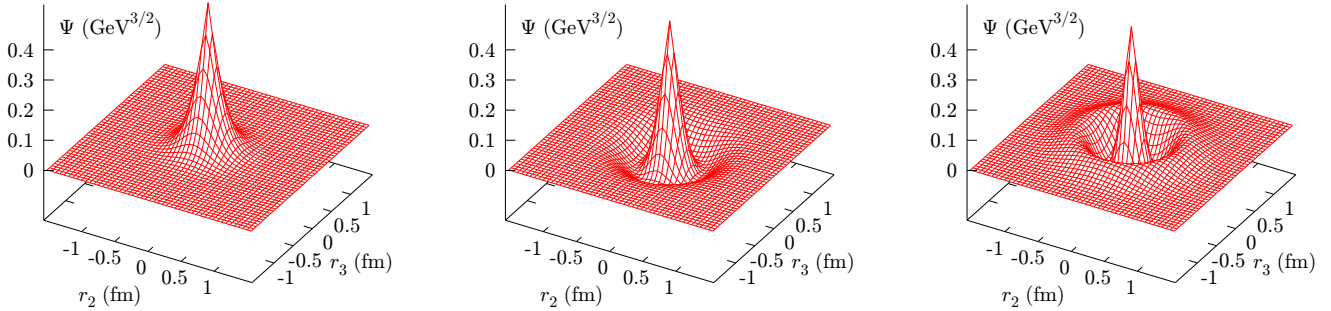


Figure 1: The shape-functions Ψ_{1S} (left), Ψ_{2S} (middle), Ψ_{3S} (right) used to calculate η_b and Υ correlators for lattices with $a = 0.0655$ fm.

2. Methodology

The lattice NRQCD Lagrangian employed in this study is exactly the same as in Refs. [40, 41]— tree-level tadpole improved, accurate up to order v^4 , but also includes v^6 spin dependent terms. For the background gauge fields we used 2 + 1-flavor gauge configurations on $48^3 \times 12$ lattices with bare gauge couplings $\beta = 6.74, 6.88, 7.03, 7.28$ and 7.596 , corresponding lattice spacings $a = 0.1088, 0.0951, 0.0825, 0.0655, 0.0493$ fm and temperatures $T = 151, 173, 199, 251$ and 334 MeV, respectively. For each gauge coupling we also carried out the corresponding vacuum $T = 0$ calculations. All gauge configurations were generated by the HotQCD collaboration [42, 43], with the physical value of the strange quark mass, and up/down quark masses corresponding to the pion mass of 160 MeV in the continuum limit. The lattice spacings, a , were determined using the r_1 scale from the static quark anti-quark potential and the value $r_1 = 0.3106(18)$ fm [44]. The mass parameter in the NRQCD Lagrangian was fixed through the kinetic mass of the η_b meson, described in detail in Ref. [40].

To calculate bottomonium correlators we used novel extended meson operators in Coulomb gauge of the form

$$O_i(\mathbf{x}, t) = \sum_{\mathbf{r}} \Psi_i(\mathbf{r}) \bar{q}(\mathbf{x} + \mathbf{r}, t) \Gamma q(\mathbf{x}, t). \quad (1)$$

The different choices of Γ used in this work can be found in Table 1 of Ref. [40]. The index i refers to the different states in a given channel, e.g., 1S, 2S, 3S etc. The shape-functions Ψ_i were obtained by solving the discretized Schrodinger equation with a Cornell potential on a 3-dimensional lattice having a lattice spacing and a volume exactly the same as that of the corresponding QCD background. Spin interactions were neglected. For the lattice Schrodinger equation we used an $O(a^2)$ -improved Laplace operator. For the Cornell potential the string tension was chosen to be $(468 \text{ MeV})^2$, and the Coulomb part was computed at tree-level in lattice perturbation theory for the Symanzik-improved lattice gluon action with a fixed strong coupling constant $\alpha_S = 0.24$. The bottom-quark mass was set to $m_b = 4.676$ GeV. More details can be found in the Appendix D of Ref. [41]. The Ψ 's used for calculations of η_b and Υ correlators for lattices with $a = 0.0655$ fm are shown in Fig. 1.

Since Ψ_i is a good approximation for the wave-function of the i^{th} vacuum bottomonium, as expected, the corresponding operator O_i was found to have a good overlap with the i^{th} state. However, the off-diagonal correlators, $G_{ij}(t) = \langle O_i(t) O_j^\dagger(0) \rangle$ for $i \neq j$, were found to be non-zero, though small. Thus, we resorted to the variational analysis by considering linear combinations $\tilde{O}_\alpha = \Omega_{\alpha j} O_j$ such that $\langle \tilde{O}_\alpha(t) \tilde{O}_\beta^\dagger(0) \rangle \propto \delta_{\alpha, \beta}$. The matrices $\Omega_{\alpha j}$ were obtained using the generalized eigenvalue problem [45–49] $G_{ij}(t) \Omega_{\alpha j} = \lambda_\alpha(t, t_0) G_{ij}(t_0) \Omega_{\alpha j}$. We calculated the correlators of optimized operators $C_\alpha(t) = \langle \tilde{O}_\alpha(t) \tilde{O}_\alpha^\dagger(0) \rangle$ for 1S, 1P, 2S, 2P and 3S. When calculating $\Omega_{\alpha j}$, the value of t was chosen such that it corresponds to physical extent $\tau = t \cdot a \simeq 0.5$ fm and t_0 was chosen to be $\tau = 0$ fm. Choosing t_0/a to be 1 or 2 does not change the results significantly.

3. Results

3.1. Vacuum case

In Fig. 2 we show some examples of the effective masses, $aM_{\text{eff}}(t) = \ln[C_\alpha(t)/C_\alpha(t+a)]$, at $T = 0$. Those were found to reach a plateau for $\tau \simeq 0.4$ fm for all states. For the excited states we see stable plateaus up to τ of around 1.2 fm, beyond which signal deteriorated. Performing single-exponential fits in the plateau region we extracted the energy levels of different bottomonium states. Since the NRQCD energy levels contain an additional lattice spacing dependent constant, the differences of these energy levels have the physical interpretation of mass differences of different bottomonium states. Thus, in this work we set the spin-average energy of 1S bottomonium, $\bar{E}_{1S} = (E_{\eta_b} + 3E_\Upsilon)/4$, to be the zero of the mass/energy, and quote masses/energies of the rest of the bottomonium states with respect to these baselines for each lattice spacing. (Note that, in Ref. [40] this baseline was set by the η_b energy level.) The reason being \bar{E}_{1S} remains unaffected by the spin-spin interaction, which is difficult to reproduce accurately using tree-level NRQCD Lagrangian used in this study. The energy differences show a very mild dependence on the lattice spacing, and in most cases can be fitted with a constant to obtain our final estimate for the energy differences. The only exceptions are the energy of

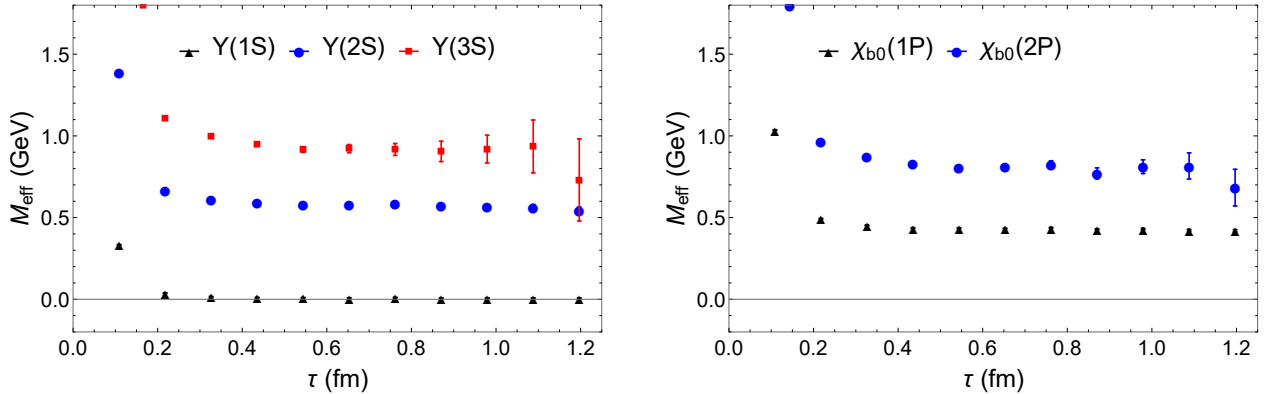


Figure 2: The effective masses, M_{eff} , at $T = 0$ for different Υ (left) and χ_{b0} (right) states calculated on the lattice with $a = 0.109$ fm.

χ_{b0} and the 2S hyperfine splitting, where the a -dependence cannot be neglected. We also fitted the resulting energy differences with a constant plus a term proportional to a^2 to remove the remaining discretization effects, this resulted in small differences in the central value but larger statistical errors for the final estimate. We used this procedure to compare with the experimental results, except for 3S state, where it gives too large statistical errors. The comparison of the zero temperature results on the mass differences with the experimental results from the Particle Data Group (PDG) [50] is shown in Table 1. We see very good agreement between our lattice NRQCD calculations and the experimental results within the estimated errors in most cases. The only exception is the $\chi_{b0}(1P)$ state, where a small tension between our result and the PDG value is observed. Using the result for the 3S hyperfine splitting we can also predict the mass of the $\eta_b(3S)$ state to be 10341.8 ± 6.2 MeV, that has not yet been observed experimentally.

3.2. In-medium case

In NRQCD the spectral function, $\rho(\omega, T)$, is related to the Euclidean time correlation function:

$$C_\alpha(\tau, T) = \int_{-\infty}^{\infty} d\omega \rho_\alpha(\omega, T) e^{-\omega\tau}. \quad (2)$$

Here, α labels the bottomonium operator of interest. Bottomonium states correspond to peaks in the spectral function having some in-medium width. At large ω many states contribute to the spectral function, forming a continuum. Therefore, we can write the spectral function as

$$\rho_\alpha(\omega, T) = \rho_\alpha^{\text{med}}(\omega, T) + \rho_\alpha^{\text{high}}(\omega), \quad (3)$$

with the second term parameterizing the continuum part of the spectral function. In the zero-temperature limit $\rho_\alpha^{\text{med}}(\omega, T) = A_\alpha \delta(\omega - M_\alpha)$, M_α being the mass of the corresponding bottomonium state. Here we note that the use of extended operators reduces the relative contribution of $\rho_\alpha^{\text{high}}$ [51, 52]. For this reason the effective masses in Fig. 2 approach a plateau at relatively small τ . The continuum

| state | ΔM [MeV] | $\Delta M(PDG)$ [MeV] |
|-----------------|------------------|-----------------------|
| $\Upsilon(3S)$ | 906.0(25.0)(5.2) | 910.3(0.7) |
| $h_b(2P)$ | 804.4(35.8)(4.7) | 814.9(1.3) |
| $\chi_{b2}(2P)$ | 809.2(36.2)(4.7) | 823.8(0.9) |
| $\chi_{b1}(2P)$ | 802.2(34.9)(4.7) | 810.6(0.7) |
| $\chi_{b0}(2P)$ | 786.8(32.7)(4.6) | 787.6(0.8) |
| $\Upsilon(2S)$ | 582.7(9.8)(3.4) | 578.4(0.6) |
| $h_b(1P)$ | 454.5(4.7)(2.6) | 454.4(0.9) |
| $\chi_{b2}(1P)$ | 463.3(4.8)(2.7) | 467.3(0.6) |
| $\chi_{b1}(1P)$ | 448.9(4.6)(2.6) | 447.9(0.6) |
| $\chi_{b0}(1P)$ | 421.3(4.7)(2.4) | 414.5(0.7) |
| hyperfine(3S) | 13.4(6.2)(0.1) | NA |
| hyperfine(2S) | 24.1(1.0)(0.1) | 24.5(4.5) |

Table 1: Comparisons of mass differences ΔM (in units of MeV) of various bottomonium states with respect to the 1S spin-averaged mass obtained from our lattice calculations with that from PDG [50]. The last two rows show the 2S and 3S hyperfine splitting. The second error in our results corresponds to the uncertainty of the r_1 scale.

part, $\rho_\alpha^{\text{high}}(\omega)$, is expected to be temperature independent. This was seen to fit with our calculation, as the temperature dependence of $C_\alpha(\tau, T)$ for $\tau \lesssim 0.3$ fm was very small, with the small difference being in agreement with changes due to the medium. Thus, following Ref. [40], for each lattice spacing we can identify the contribution of $\rho_\alpha^{\text{high}}(\omega)$ to the correlator, $C_\alpha^{\text{high}}(\tau)$, as

$$C_\alpha(\tau, T = 0) = A_\alpha e^{-M_\alpha \tau} + C_\alpha^{\text{high}}(\tau). \quad (4)$$

Here, A_α and M_α are the amplitude and mass of the corresponding bottomonium state, and $C_\alpha^{\text{high}}(\tau)$ is the Laplace transform of $\rho_\alpha^{\text{high}}$. Using the single-exponential fits to the vacuum correlators for $\tau \gtrsim 0.6$ fm, and subtracting off this contribution from $C_\alpha(\tau, T = 0)$ we isolated $C_\alpha^{\text{high}}(\tau)$ for each value of β . Further, following Ref. [40], for each temperature we then defined the continuum-subtracted correlator as

$$C_\alpha^{\text{sub}}(\tau, T) = C_\alpha(\tau, T) - C_\alpha^{\text{high}}(\tau). \quad (5)$$

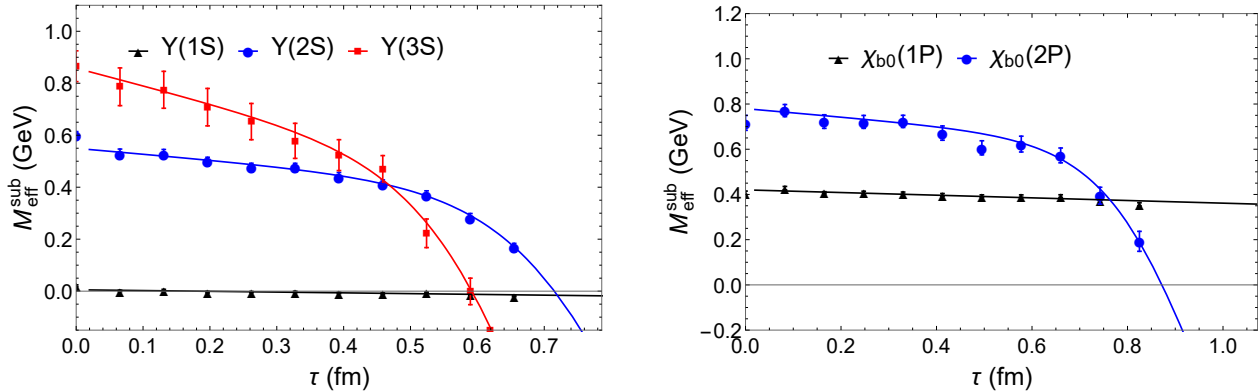


Figure 3: Continuum-subtracted effective masses, $M_{\text{eff}}^{\text{sub}}$, of Υ states at $T = 251$ MeV (left) and χ_{b0} states at $T = 199$ MeV (right).

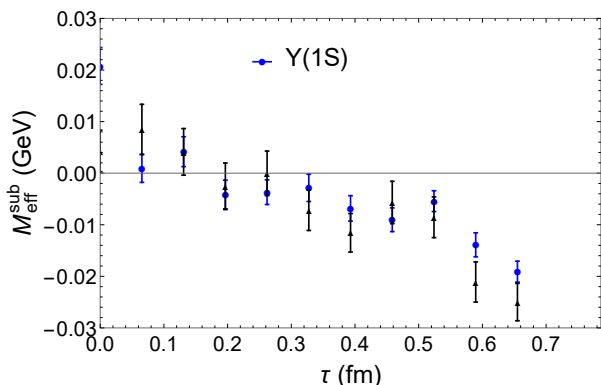


Figure 4: Comparison of the continuum-subtracted effective mass, $M_{\text{eff}}^{\text{sub}}$, of $\Upsilon(1S)$ at $T = 251$ MeV obtained in this study (circle) and using Gaussian extended source (triangle) of Ref. [40].

Thus, the continuum-subtracted correlator, $C_{\alpha}^{\text{sub}}(\tau, T)$, is mostly sensitive to $\rho_{\alpha}^{\text{med}}(\omega, T)$, encoding the in-medium bottomonium properties. We then studied the in-medium bottomonium properties using the continuum-subtracted effective masses,

$$aM_{\text{eff}}^{\text{sub}}(\tau, T) = \ln(C_{\alpha}^{\text{sub}}(\tau, T)/C_{\alpha}^{\text{sub}}(\tau + a, T)). \quad (6)$$

In Fig. 3 we show typical examples of $M_{\text{eff}}^{\text{sub}}$ as a function of τ — for the Υ states at $T = 251$ MeV and for the χ_{b0} states at $T = 199$ MeV. At small τ , $M_{\text{eff}}^{\text{sub}}$ are approximately equal to the vacuum masses. As τ increases, we see an approximately linear decrease of $M_{\text{eff}}^{\text{sub}}$. Finally, for $\tau \simeq 1/T$ we see a rapid drop-off. Similar behaviors of $M_{\text{eff}}^{\text{sub}}$ for the ground states were also observed in the previous study using Gaussian smeared meson operators [40]. As discussed in Ref. [40], the slope of the linear decrease of $M_{\text{eff}}^{\text{sub}}$ can be understood in terms of a thermal width. We see that the slope is larger for higher excited bottomonium states, i.e., the thermal width of different bottomonium states follows the expected hierarchy of their sizes. Higher excited states have larger size and therefore are more affected by the medium, leading to larger width. The behavior of the effective masses at $\tau \simeq 1/T$ is related to the tail of the spectral function at small ω ,

and may depend on the choice of the meson operator [40]. Therefore, it is important to compare the results on the subtracted effective masses obtained with different meson operators. In Fig. 4 we compare $M_{\text{eff}}^{\text{sub}}$ of subtracted $\Upsilon(1S)$ at $T = 251$ MeV with the corresponding results obtained with Gaussian smeared sources of Ref. [40]. Good agreement was found between the present results and those obtained of Ref. [40], especially for $\tau \approx 1/T$. Therefore, our conclusion regarding the in-medium modification of the spectral functions is not affected by the choices of meson operators. For $\tau \simeq 1/T$ we see a smaller drop-off in $M_{\text{eff}}^{\text{sub}}$ compared to that observed in Ref. [40]. Thus, the small- ω tail of the spectral functions plays a less prominent role here. We found that the behaviors of $M_{\text{eff}}^{\text{sub}}$ for $\eta_b(nS)$ are very similar to that of $\Upsilon(nS)$, and that of $\chi_{b1}(nP)$, $\chi_{b2}(nP)$ and $h_b(nP)$ are very similar to that of $\chi_{b0}(nP)$.

As introduced in Ref. [40], the simplest theoretically motivated parameterization of the in-medium spectral function that can describe the generic behavior of $M_{\text{eff}}^{\text{sub}}$ observed here is as follows

$$\rho_{\alpha}^{\text{med}}(\omega, T) = A_{\alpha}^{\text{cut}}(T) \delta(\omega - \omega_{\alpha}^{\text{cut}}(T)) + A_{\alpha}(T) \exp\left(-\frac{[\omega - M_{\alpha}(T)]^2}{2\Gamma_{\alpha}^2(T)}\right). \quad (7)$$

The first term in the above equation provides a simple parameterization of the low- ω tail of the spectral function. As explained in Ref. [40], this tail is important for understanding the behavior of the effective masses around $\tau \simeq 1/T$. The second term gives rise to the linear behavior in τ of $M_{\text{eff}}^{\text{sub}}$, with the slope given by Γ_{α}^2 . For each temperature, we fitted $M_{\text{eff}}^{\text{sub}}(\tau)$ with the Ansatz given by Eq. (7), and using Eqs. (2), (6), to determine the in-medium masses, $M_{\alpha}(T)$, and width, $\Gamma_{\alpha}(T)$, of different bottomonium states. Since the tail of the spectral function plays a less prominent role in the present study, for $T \leq 173$ MeV and all temperatures for Υ 1S, we performed fits, setting $A_{\alpha}^{\text{cut}} = 0$, and omitting 1-3 data points for the largest values of τ . Only for higher temperatures was the term proportional to A_{α}^{cut} included. We generally find good fits with χ^2 divided by degrees of freedom being

around 0.5. In some cases the data points fluctuate more than the size of the estimated errors. Examples of such cases include $\Upsilon(1S)$ and also χ_{b0} at 199 MeV, as can be seen on the right in Fig. 3. In these cases we found that χ^2 divided by degrees of freedom was around 2. The fit still seem to work nicely, so it is most likely the errors that were a bit too small.

The change of the in-medium mass parameter compared to the vacuum mass (M_α^0), $\Delta M_\alpha(T) = M_\alpha(T) - M_\alpha^0$, and width parameter, $\Gamma_\alpha(T)$, are shown in Figs. 5 and 6, respectively. The in-medium masses of different states obtained from the fits turned out to be very similar to the vacuum masses. In fact, we do not see any statistically significant deviations from the $T = 0$ results. On the other hand, $\Gamma_\alpha(T)$ shows a clear increase with increasing temperature. For large enough temperatures, $\Gamma_\alpha(T)$ appears to approximately rise linearly with T . Nearly for the entire T -range, the in-medium width was found to follow the sequential hierarchical pattern according to the increasing sizes of the bottomonium states: $\Gamma_{1S}(T) < \Gamma_{1P}(T) < \Gamma_{2S}(T) < \Gamma_{2P}(T) < \Gamma_{3S}(T)$. Moreover, $\Gamma_{3S} \gtrsim M_{3S} - M_{2S}$ and $\Gamma_{2P} \gtrsim M_{2P} - M_{1P}$ for $T \gtrsim 200$ MeV. As a result, at these temperatures $2S$ and $3S$, as well as the $1P$ and $2P$ states will together appear as broad structures in their respective spectral functions. These observations lead us to conclude that, similar to what have been observed in the experiments [18, 19], for $T \gtrsim 200$ MeV it will become difficult to individually identify the $2S$, $3S$, $1P$ and $2P$ states within the experimentally measured line shapes of the invariant-mass distributions.

Lastly, we address the question to what extent the estimated thermal widths of bottomonium states depend on the model for the spectral function used to interpret our lattice QCD results presented here. Since $M_{\text{eff}}^{\text{sub}}(\tau)$ show a linear in τ behavior and we do not observe any significant thermal mass shift, following Ref. [40], we also used the following model for the spectral function:

$$\begin{aligned} \rho_\alpha^{\text{med}}(\omega, T) = & A_\alpha^{\text{cut}}(T) \delta(\omega - \omega_\alpha^{\text{cut}}(T)) \\ & + \delta(\omega - M_\alpha^0 + \Delta_\alpha(T)) \\ & + \delta(\omega - M_\alpha^0) \\ & + \delta(\omega - M_\alpha^0 - \Delta_\alpha(T)). \end{aligned} \quad (8)$$

Here, M_α^0 is the vacuum bottomonium mass, and the parameters A_α^{cut} and $\omega_\alpha^{\text{cut}}$ describe the low- ω tail of the spectral function. For $T \leq 173$ MeV again we used $A_\alpha^{\text{cut}} = 0$. The equivalent thermal width in this case is $\Gamma_\alpha(T) = \sqrt{2/3}\Delta_\alpha(T)$. Carrying out fits with the above Ansatz we obtained thermal widths that, as shown in Fig. 6, within errors, agreed with the ones obtained by using the Gaussian Ansatz. Therefore, our estimates of thermal width do not depend very much on the precise functional form of the fit Ansatz.

4. Conclusion

For the very first time, we studied in-medium properties up to $3S$ and $2P$ excited bottomonium states using lattice QCD at temperatures $T \simeq 150 - 350$ MeV. This lattice QCD study was made possible through the introduction of novel bottomonium operators within the lattice NRQCD framework, and implementation of a variational analysis based on these novel operators. We found that the effective masses constructed out of the continuum-subtracted bottomonium correlation functions drop off linearly in Euclidean time. We argued that the behaviors of the continuum-subtracted effective masses can be understood in terms of a couple of theoretically-motivated, simple models of the bottomonium spectral functions. For all of the models considered, we found indications of thermal broadening of bottomonium states in QGP. For the entire temperature range, the magnitudes of the thermal broadening were found to follow the expected sequential hierarchical pattern according to the increasing sizes of the bottomonium states. Further, we found that for $T \gtrsim 200$ MeV the thermal broadening of the $2S$, $3S$, $1P$ and $2P$ states becomes large enough that it would be difficult to identify these states separately within the corresponding spectral functions.

Acknowledgments

This material is based upon work supported by the U.S. Department of Energy, Office of Science, Office of Nuclear Physics: (i) Through the Contract No. DE-SC0012704; (ii) Through the Scientific Discovery through Advance Computing (SciDAC) award Computing the Properties of Matter with Leadership Computing Resources. (iii) Stefan Meinel acknowledges support by the U.S. Department of Energy, Office of Science, Office of High Energy Physics under Award Number DE-SC0009913.

This research used awards of computer time: (i) Provided by the USQCD consortium at its Fermi National Laboratory, Brookhaven National Laboratory and Jefferson Laboratory computing facilities; (ii) Provided by the INCITE program at Argonne Leadership Computing Facility, a U.S. Department of Energy Office of Science User Facility operated under Contract No. DE-AC02-06CH11357; (ii) Provided by the ALCC program at National Energy Research Scientific Computing Center, a U.S. Department of Energy Office of Science User Facility operated under Contract No. DE-AC02-05CH11231; (iii) Provided by the INCITE programs at Oak Ridge Leadership Computing Facility, a DOE Office of Science User Facility operated under Contract No. DE-AC05-00OR22725.

References

- [1] T. Matsui, H. Satz, J/ψ Suppression by Quark-Gluon Plasma Formation, Phys. Lett. B178 (1986) 416–422. doi:10.1016/0370-2693(86)91404-8.

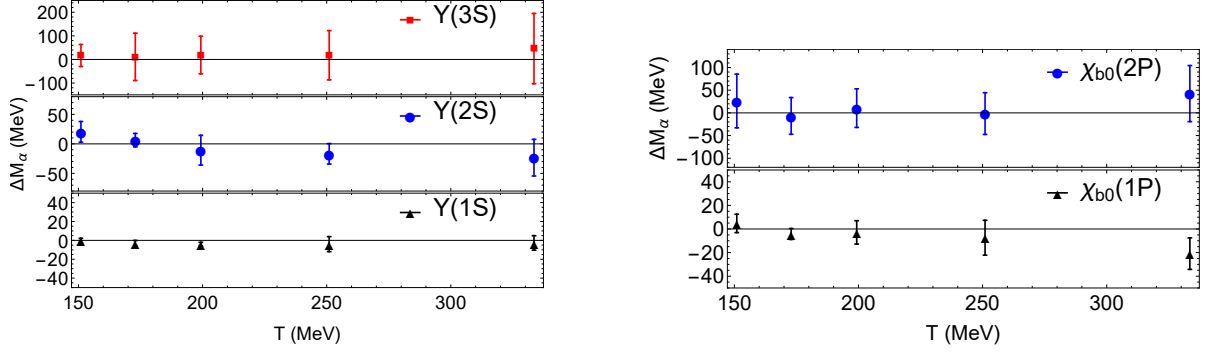


Figure 5: The change of the in-medium mass compared to the vacuum mass, $\Delta M_\alpha = M_\alpha(T) - M_\alpha^0$, for the Υ (left) and χ_{b0} states (right) as function of the temperature.

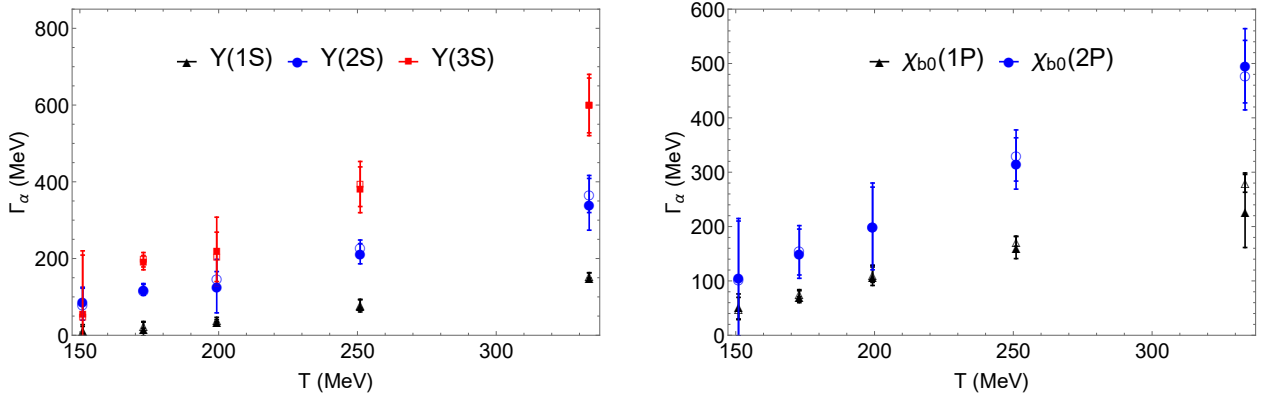


Figure 6: Thermal width, Γ_α , of Υ (left) and χ_{b0} states (right) as function of the temperature using Eq. (7) (filled) and using Eq. (8) (empty). Fit with Eq. (8) assumes $M_\alpha(T) = M_\alpha^0$ and error bars are thus slightly smaller.

- [2] F. Karsch, M. T. Mehr, H. Satz, Color Screening and Deconfinement for Bound States of Heavy Quarks, *Z. Phys. C* 37 (1988) 617. doi:10.1007/BF01549722.
- [3] S. Digal, P. Petreczky, H. Satz, Quarkonium feed down and sequential suppression, *Phys. Rev. D* 64 (2001) 094015. arXiv: hep-ph/0106017, doi:10.1103/PhysRevD.64.094015.
- [4] G. Aarts, S. Kim, M. P. Lombardo, M. B. Oktay, S. M. Ryan, D. K. Sinclair, J. I. Skullerud, Bottomonium above deconfinement in lattice nonrelativistic QCD, *Phys. Rev. Lett.* 106 (2011) 061602. arXiv:1010.3725, doi:10.1103/PhysRevLett.106.061602.
- [5] G. Aarts, C. Allton, S. Kim, M. P. Lombardo, S. M. Ryan, J. I. Skullerud, Melting of P wave bottomonium states in the quark-gluon plasma from lattice NRQCD, *JHEP* 12 (2013) 064. arXiv:1310.5467, doi:10.1007/JHEP12(2013)064.
- [6] G. Aarts, C. Allton, T. Harris, S. Kim, M. P. Lombardo, S. Ryan, J.-I. Skullerud, The bottomonium spectrum at finite temperature from $N_f = 2 + 1$ lattice QCD, *JHEP* 07 (2014) 097. arXiv:1402.6210, doi:10.1007/JHEP07(2014)097.
- [7] S. Kim, P. Petreczky, A. Rothkopf, Quarkonium in-medium properties from realistic lattice NRQCD, *JHEP* 11 (2018) 088. arXiv:1808.08781, doi:10.1007/JHEP11(2018)088.
- [8] S. Kim, P. Petreczky, A. Rothkopf, Lattice NRQCD study of S- and P-wave bottomonium states in a thermal medium with $N_f = 2 + 1$ light flavors, *Phys. Rev. D* 91 (2015) 054511. arXiv:1409.3630, doi:10.1103/PhysRevD.91.054511.
- [9] A. Bazavov, F. Karsch, Y. Maenzawa, S. Mukherjee, P. Petreczky, In-medium modifications of open and hidden strange-charm mesons from spatial correlation functions, *Phys. Rev. D* 91 (5) (2015) 054503. arXiv:1411.3018, doi:10.1103/PhysRevD.91.054503.
- [10] F. Karsch, E. Laermann, S. Mukherjee, P. Petreczky, Signatures of charmonium modification in spatial correlation functions, *Phys. Rev. D* 85 (2012) 114501. arXiv:1203.3770, doi:10.1103/PhysRevD.85.114501.
- [11] M. Laine, O. Philipsen, P. Romatschke, M. Tassler, Real-time static potential in hot QCD, *JHEP* 03 (2007) 054. arXiv: hep-ph/0611300, doi:10.1088/1126-6708/2007/03/054.
- [12] N. Brambilla, J. Ghiglieri, A. Vairo, P. Petreczky, Static quark-antiquark pairs at finite temperature, *Phys. Rev. D* 78 (2008) 014017. arXiv:0804.0993, doi:10.1103/PhysRevD.78.014017.
- [13] M. Laine, A Resummed perturbative estimate for the quarkonium spectral function in hot QCD, *JHEP* 05 (2007) 028. arXiv:0704.1720, doi:10.1088/1126-6708/2007/05/028.
- [14] Y. Burnier, M. Laine, M. Vepsalainen, Heavy quarkonium in any channel in resummed hot QCD, *JHEP* 01 (2008) 043. arXiv:0711.1743, doi:10.1088/1126-6708/2008/01/043.
- [15] A. Beraudo, J. P. Blaizot, C. Ratti, Real and imaginary-time Q anti-Q correlators in a thermal medium, *Nucl. Phys. A* 806 (2008) 312-338. arXiv:0712.4394, doi:10.1016/j.nuclphysa.2008.03.001.
- [16] P. Petreczky, C. Miao, A. Mocsy, Quarkonium spectral functions with complex potential, *Nucl. Phys. A* 855 (2011) 125-132. arXiv:1012.4433, doi:10.1016/j.nuclphysa.2011.02.028.
- [17] Y. Burnier, O. Kaczmarek, A. Rothkopf, Quarkonium at finite temperature: Towards realistic phenomenology from first principles, *JHEP* 12 (2015) 101. arXiv:1509.07366, doi:10.1007/JHEP12(2015)101.
- [18] S. Chatrchyan, et al., Indications of suppression of excited Υ states in PbPb collisions at $\sqrt{s_{NN}} = 2.76$ TeV, *Phys. Rev. Lett.* 107 (2011) 052302. arXiv:1105.4894, doi:10.1103/PhysRevLett.107.052302.

- [19] S. Chatrchyan, et al., Observation of Sequential Upsilon Suppression in PbPb Collisions, *Phys. Rev. Lett.* 109 (2012) 222301, [Erratum: *Phys. Rev. Lett.* 120, no. 19, 199903 (2018)]. [arXiv:1208.2826](#), [doi:10.1103/PhysRevLett.109.222301](#), [10.1103/PhysRevLett.120.199903](#).
- [20] V. Khachatryan, et al., Suppression of $\Upsilon(1S)$, $\Upsilon(2S)$ and $\Upsilon(3S)$ production in PbPb collisions at $\sqrt{s_{NN}} = 2.76$ TeV, *Phys. Lett. B* 770 (2017) 357–379. [arXiv:1611.01510](#), [doi:10.1016/j.physletb.2017.04.031](#).
- [21] A. M. Sirunyan, et al., Suppression of Excited Υ States Relative to the Ground State in Pb-Pb Collisions at $\sqrt{s_{NN}}=5.02$ TeV, *Phys. Rev. Lett.* 120 (14) (2018) 142301. [arXiv:1706.05984](#), [doi:10.1103/PhysRevLett.120.142301](#).
- [22] P. Wang, Γ measurements in Au+Au collisions at $\sqrt{s_{NN}} = 200$ GeV with the STAR experiment, *Nucl. Phys. A* 982 (2019) 723–726. [doi:10.1016/j.nuclphysa.2018.09.025](#).
- [23] B. Krouppa, A. Rothkopf, M. Strickland, Bottomonium suppression using a lattice QCD vetted potential, *Phys. Rev. D* 97 (1) (2018) 016017. [arXiv:1710.02319](#), [doi:10.1103/PhysRevD.97.016017](#).
- [24] X. Yao, M. Berndt, Approach to equilibrium of quarkonium in quark-gluon plasma, *Phys. Rev. C* 97 (1) (2018) 014908, [Erratum: *Phys. Rev. C* 97, no. 4, 049903 (2018)]. [arXiv:1709.03529](#), [doi:10.1103/PhysRevC.97.049903](#), [10.1103/PhysRevC.97.014908](#).
- [25] P. Petreczky, C. Young, Sequential bottomonium production at high temperatures, *Few Body Syst.* 58 (2) (2017) 61. [arXiv:1606.08421](#), [doi:10.1007/s00601-016-1188-8](#).
- [26] A. Mocsy, P. Petreczky, M. Strickland, Quarkonia in the Quark Gluon Plasma, *Int. J. Mod. Phys. A* 28 (2013) 1340012. [arXiv:1302.2180](#), [doi:10.1142/S0217751X13400125](#).
- [27] G. Aarts, et al., Heavy-flavor production and medium properties in high-energy nuclear collisions - What next?, *Eur. Phys. J. A* 53 (5) (2017) 93. [arXiv:1612.08032](#), [doi:10.1140/epja/i2017-12282-9](#).
- [28] T. Umeda, K. Nomura, H. Matsufuru, Charmonium at finite temperature in quenched lattice QCD, *Eur. Phys. J. C* 39S1 (2005) 9–26. [arXiv:hep-lat/0211003](#), [doi:10.1140/epjcd/s2004-01-002-1](#).
- [29] S. Datta, F. Karsch, P. Petreczky, I. Wetzorke, A Study of charmonium systems across the deconfinement transition, *Nucl. Phys. Proc. Suppl.* 119 (2003) 487–489, [487(2002)]. [arXiv:hep-lat/0208012](#), [doi:10.1016/S0920-5632\(03\)01591-3](#).
- [30] F. Karsch, S. Datta, E. Laermann, P. Petreczky, S. Stickan, I. Wetzorke, *Nucl. Phys. A* 715 (2003) 701–704. [arXiv:hep-ph/0209028](#), [doi:10.1016/S0375-9474\(02\)01470-7](#).
- [31] S. Datta, F. Karsch, P. Petreczky, I. Wetzorke, Behavior of charmonium systems after deconfinement, *Phys. Rev. D* 69 (2004) 094507. [arXiv:hep-lat/0312037](#), [doi:10.1103/PhysRevD.69.094507](#).
- [32] M. Asakawa, T. Hatsuda, J/ψ and $\eta(c)$ in the deconfined plasma from lattice QCD, *Phys. Rev. Lett.* 92 (2004) 012001. [arXiv:hep-lat/0308034](#), [doi:10.1103/PhysRevLett.92.012001](#).
- [33] A. Jakovac, P. Petreczky, K. Petrov, A. Velytsky, Quarkonium correlators and spectral functions at zero and finite temperature, *Phys. Rev. D* 75 (2007) 014506. [arXiv:hep-lat/0611017](#), [doi:10.1103/PhysRevD.75.014506](#).
- [34] H. Ohno, S. Aoki, S. Ejiri, K. Kanaya, Y. Maezawa, H. Saito, T. Umeda, Charmonium spectral functions with the variational method in zero and finite temperature lattice QCD, *Phys. Rev. D* 84 (2011) 094504. [arXiv:1104.3384](#), [doi:10.1103/PhysRevD.84.094504](#).
- [35] H. T. Ding, A. Francis, O. Kaczmarek, F. Karsch, H. Satz, W. Soeldner, Charmonium properties in hot quenched lattice QCD, *Phys. Rev. D* 86 (2012) 014509. [arXiv:1204.4945](#), [doi:10.1103/PhysRevD.86.014509](#).
- [36] H.-T. Ding, O. Kaczmarek, S. Mukherjee, H. Ohno, H. T. Shu, Stochastic reconstructions of spectral functions: Application to lattice QCD, *Phys. Rev. D* 97 (9) (2018) 094503. [arXiv:1712.03341](#), [doi:10.1103/PhysRevD.97.094503](#).
- [37] G. Aarts, C. Allton, S. Kim, M. P. Lombardo, M. B. Oktay, S. M. Ryan, D. K. Sinclair, J. I. Skullerud, What happens to the Υ and η_b in the quark-gluon plasma? Bottomonium spectral functions from lattice QCD, *JHEP* 11 (2011) 103. [arXiv:1109.4496](#), [doi:10.1007/JHEP11\(2011\)103](#).
- [38] G. Aarts, C. Allton, S. Kim, M. P. Lombardo, M. B. Oktay, S. M. Ryan, D. K. Sinclair, J.-I. Skullerud, S wave bottomonium states moving in a quark-gluon plasma from lattice NRQCD, *JHEP* 03 (2013) 084. [arXiv:1210.2903](#), [doi:10.1007/JHEP03\(2013\)084](#).
- [39] A. Mocsy, P. Petreczky, Can quarkonia survive deconfinement?, *Phys. Rev. D* 77 (2008) 014501. [arXiv:0705.2559](#), [doi:10.1103/PhysRevD.77.014501](#).
- [40] R. Larsen, S. Meinel, S. Mukherjee, P. Petreczky, Thermal broadening of bottomonia: Lattice nonrelativistic QCD with extended operators, *Phys. Rev. D* 100 (2019) 074506. [arXiv:1908.08437](#), [doi:10.1103/PhysRevD.100.074506](#).
- [41] S. Meinel, Bottomonium spectrum at order v^6 from domain-wall lattice QCD: Precise results for hyperfine splittings, *Phys. Rev. D* 82 (2010) 114502. [arXiv:1007.3966](#), [doi:10.1103/PhysRevD.82.114502](#).
- [42] A. Bazavov, et al., The chiral and deconfinement aspects of the QCD transition, *Phys. Rev. D* 85 (2012) 054503. [arXiv:1111.1710](#), [doi:10.1103/PhysRevD.85.054503](#).
- [43] A. Bazavov, et al., Equation of state in $(2+1)$ -flavor QCD, *Phys. Rev. D* 90 (2014) 094503. [arXiv:1407.6387](#), [doi:10.1103/PhysRevD.90.094503](#).
- [44] A. Bazavov, et al., Results for light pseudoscalar mesons, *PoS LATTICE2010* (2010) 074. [arXiv:1012.0868](#).
- [45] K. Nochi, T. Kawanai, S. Sasaki, Bethe-Salpeter wave functions of $\eta_c(2S)$ and $\psi(2S)$ states from full lattice QCD, *Phys. Rev. D* 94 (11) (2016) 114514. [arXiv:1608.02340](#), [doi:10.1103/PhysRevD.94.114514](#).
- [46] C. Michael, Adjoint Sources in Lattice Gauge Theory, *Nucl. Phys. B* 259 (1985) 58–76. [doi:10.1016/0550-3213\(85\)90297-4](#).
- [47] M. Luscher, U. Wolff, How to Calculate the Elastic Scattering Matrix in Two-dimensional Quantum Field Theories by Numerical Simulation, *Nucl. Phys. B* 339 (1990) 222–252. [doi:10.1016/0550-3213\(90\)90540-T](#).
- [48] B. Blossier, M. Della Morte, G. von Hippel, T. Mendes, R. Sommer, On the generalized eigenvalue method for energies and matrix elements in lattice field theory, *JHEP* 04 (2009) 094. [arXiv:0902.1265](#), [doi:10.1088/1126-6708/2009/04/094](#).
- [49] K. Orginos, D. Richards, Improved methods for the study of hadronic physics from lattice QCD, *J. Phys. G* 42 (3) (2015) 034011. [doi:10.1088/0954-3899/42/3/034011](#).
- [50] M. Tanabashi, et al., *Phys. Rev. D* 98 (2018) 030001. [doi:10.1103/PhysRevD.98.030001](#), [link]. URL <https://link.aps.org/doi/10.1103/PhysRevD.98.030001>
- [51] I. Wetzorke, F. Karsch, E. Laermann, P. Petreczky, S. Stickan, Meson spectral functions at finite temperature, *Nucl. Phys. Proc. Suppl.* 106 (2002) 510–512. [arXiv:hep-lat/0110132](#), [doi:10.1016/S0920-5632\(01\)01763-7](#).
- [52] S. Stickan, F. Karsch, E. Laermann, P. Petreczky, Free meson spectral functions on the lattice, *Nucl. Phys. Proc. Suppl.* 129 (2004) 599–601, [599(2003)]. [arXiv:hep-lat/0309191](#), [doi:10.1016/S0920-5632\(03\)02654-9](#).